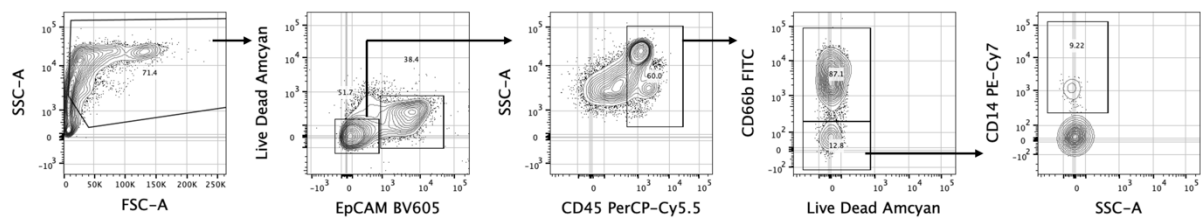


## Supplementary information

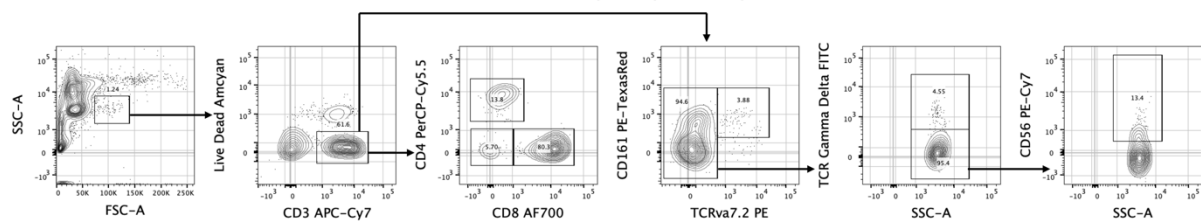
**a.**

### Myeloid panel gating strategy



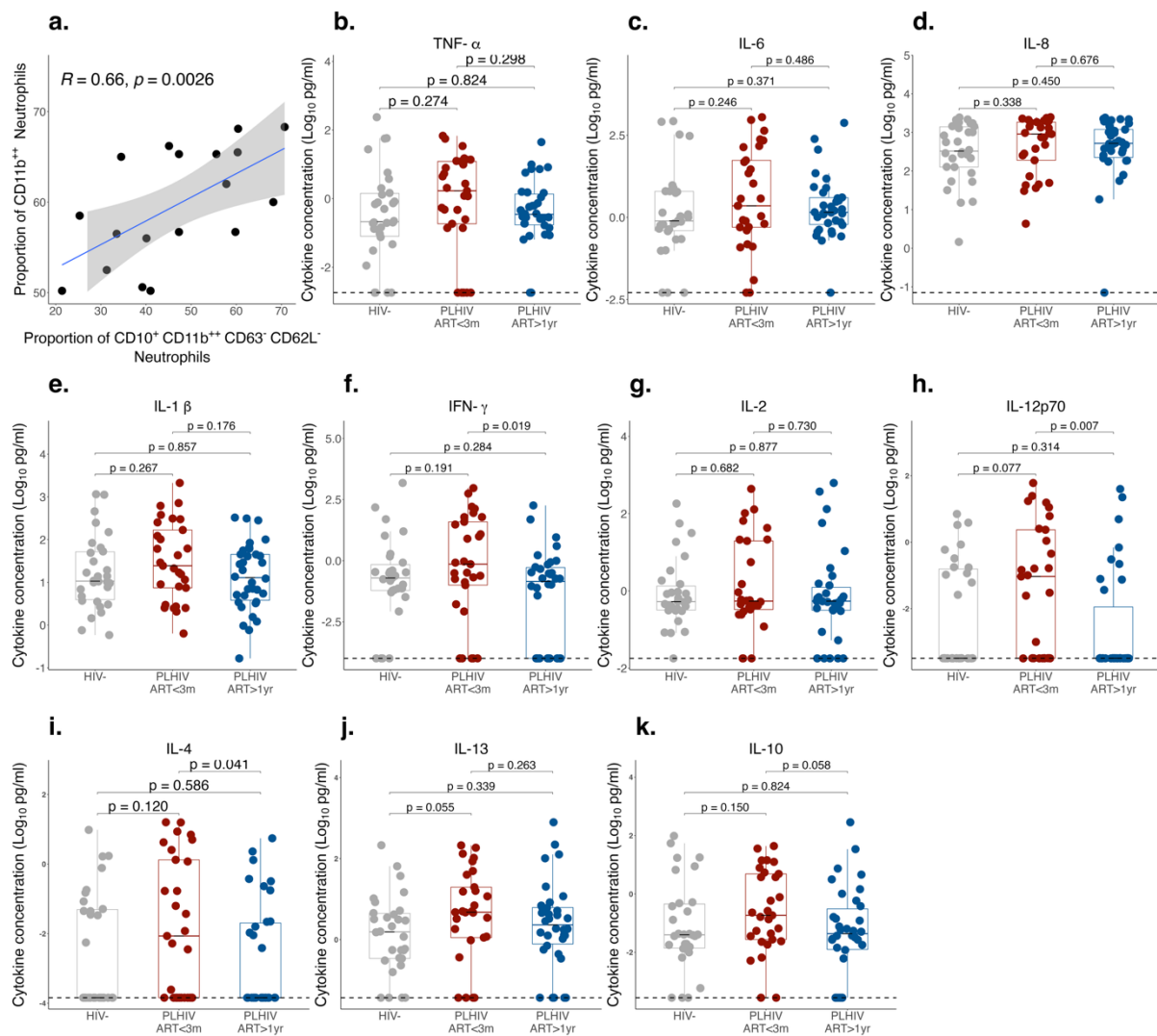
**b.**

### T cell panel gating strategy



**Supplementary Figure S1. Flow cytometry gating strategy for nasal immune cell populations.**

Nasal mucosal cells were stained with a panel of fluorescence-conjugated antibodies and analyzed by flow cytometry to define major immune cell subsets. **a**, Gating strategy for identifying myeloid cells, including neutrophils (CD66b<sup>+</sup>) and monocytes (CD14<sup>+</sup>). **b**, Gating strategy for conventional T cells (CD3<sup>+</sup>CD4<sup>+</sup>, CD3<sup>+</sup>CD8<sup>+</sup>) and innate-like T cells, including mucosal-associated invariant T (MAIT) cells (CD3<sup>+</sup>CD161<sup>+</sup>TCRVα7.2<sup>+</sup>), γδ T cells (CD3<sup>+</sup>TCRγδ<sup>+</sup>), and natural killer T (NKT) cells (CD3<sup>+</sup>CD56<sup>+</sup>).



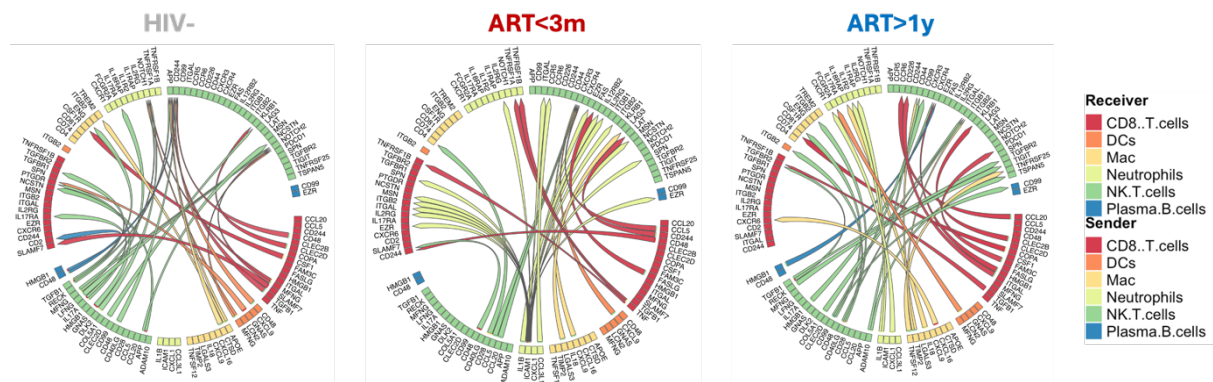
**Supplementary Figure S2. Nasal cytokine concentrations across study groups.**

Proinflammatory cytokines were measured in nasal lining fluid using a multiplex Mesoscale Discovery (MSD) panel. Samples were collected using nasosorption filters and analyzed across three study groups: HIV-uninfected adults (HIV- adults,  $n=30$ ), PLHIV on ART for <3 months (PLHIV-ART<3m,  $n=29$ ), and PLHIV on ART for >1 year (PLHIV-ART>1yr,  $n=34$ ). **a**, Scatter plot showing correlation between the proportion of nasal CD11b<sup>++</sup> neutrophils and the proportion of CD10<sup>+</sup>CD11b<sup>++</sup>CD63<sup>-</sup>CD62L<sup>-</sup> neutrophils. **b-k**, Concentrations of neutrophil chemo-attractants: TNF-α, IL-6, IL-8, and IL-1β. **f-j**, Adaptive cytokines: IFN-γ, IL-2, IL-12p70, IL-4, and IL-13. **h**, Anti-inflammatory cytokine IL-10. Box plots show the interquartile range (25<sup>th</sup> to 75<sup>th</sup> percentiles). The bold horizontal line inside each boxplot indicated the median. Whiskers extend to the smallest and largest values within 1.5x the interquartile range (IQR) from the

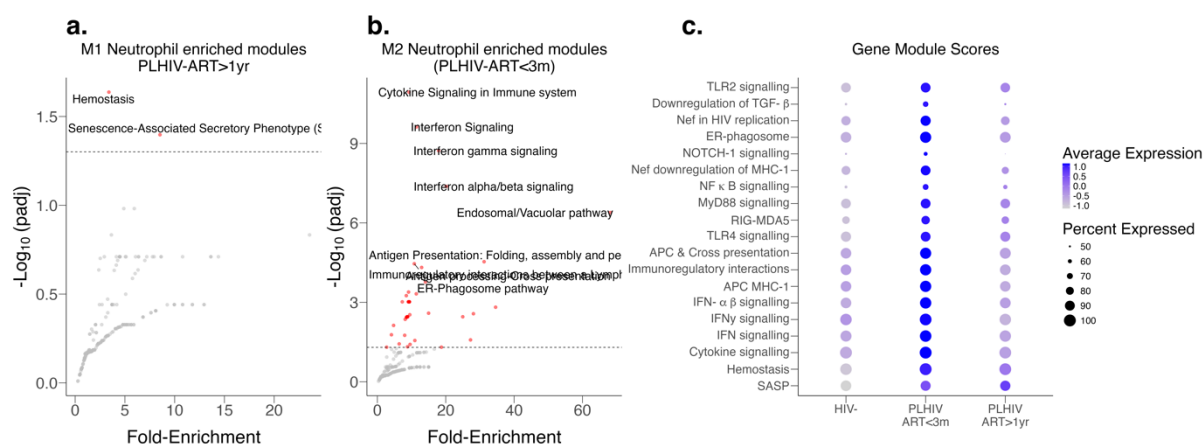
lower and upper quartiles, respectively. Individual points beyond the whiskers denote outliers. Statistical significance was assessed using two-sided Wilcoxon rank-sum tests;  $P < 0.05$  was considered significant.

**Supplementary Table S1: Demographic characteristics of participants included in the single cell analysis dataset.** Table shows the demographics characteristics of the study participants in this manuscript. median and interquartile range are show (Median (Q1, Q3) for all the continuous variables. Number of observations and proportions are shown for all categorical variables (n(%)). Kruskal-Wallis ranks sum test was used to compare the continuous variables across the study groups. Pearson's Chi-squared test and Fisher's exact test were used to compare the differences in the categorical variables across the study groups. nasal respiratory viruses\* measured included Influenza A virus, Influenza B virus, Influenza C virus, Parainfluenza virus, Respiratory syncytial virus, Rhinovirus, Adenovirus, Human metapneumovirus, Enterovirus, Human bocavirus and human parechovirus.

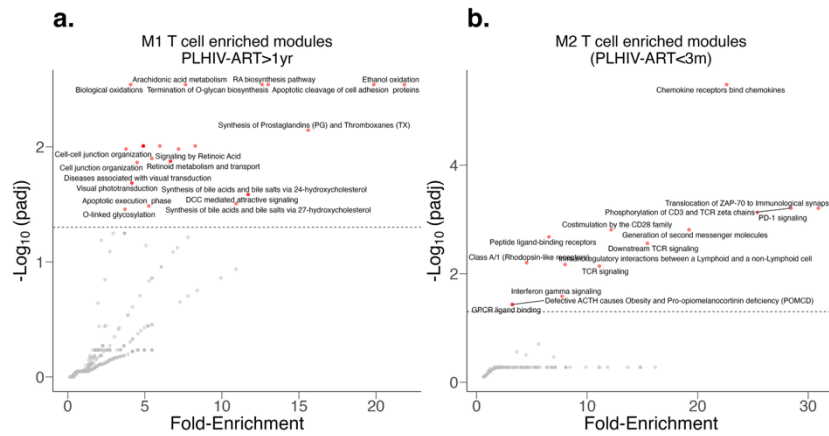
Characteristic	HIV- n=3	PLHIV-ART<3m n=3	PLHIV-ART>1yr n=5
Age (years)	28 (28,32)	26 (25,26.5)	34 (27,34)
Sex			
Male	2 (67%)	2 (67%)	2 (40%)
Female	1 (33%)	1 (33%)	3 (60%)
Blood HIV Viral Load			
Detected		1 (33%)	0 (0%)
Undetected		2 (67%)	5 (100%)
Nasal HIV viral load			
Undetected		3 (100%)	5 (100%)
Nasal respiratory viruses*			
Undetected	3 (100%)	3 (100%)	5 (100%)



**Supplementary Figure S3. Prioritised intercellular communication networks in the nasal mucosa.** Cell-to-cell communication analysis was performed using the Multinichenet package on single-cell RNA sequencing data from nasal mucosal samples across all study groups. Circos plots illustrating significant Immune cell-to-Immune cell communication networks in HIV-uninfected adults (HIV-), PLHIV on ART for <3 months (ART<3m), and PLHIV on ART for >1 year (ART>1yr). Shown are top 30-ranked ligand–receptor pairs with holm adjusted  $P < 0.05$  and expression in >10% of cells. Cell type abbreviations: CD8+.T.cells, CD8+ T cells; DCs, dendritic cells; Mac, macrophages; NK.T.cells, natural killer T cells.



**Supplementary Figure S4. Functional pathway enrichment and module scoring in neutrophil gene co-expression networks.** Pathway enrichment analysis was performed on neutrophil-specific gene co-expression modules identified using the CEMiTool package. **a-b**, Volcano plots of significantly enriched Reactome pathways for **a**, Module 1 (M1), predominantly enriched in PLHIV-ART>1yr, and **b**, Module 2 (M2), enriched in PLHIV-ART<3m. Only pathways with adjusted  $P < 0.05$  are shown. **c**, Dot plot displaying gene module scores for neutrophils, calculated across all significant M1 and M2 pathways using the AddModuleScore function in Seurat. Module scores reflect the relative expression of genes comprising each enriched pathway. Statistical significance was determined using holm adjusted  $P < 0.05$ . Abbreviations:  $-\log_{10}(\text{padj})$ ,  $-\log_{10}$  holm adjusted p-value



**Supplementary Figure S5. Functional pathway enrichment in T cells gene co-expression networks.** Pathway enrichment analysis was performed on T cell-specific gene co-expression modules identified using the CEMiTool package. **a-b**, Volcano plots of significantly enriched Reactome pathways for **a**, Module 1 (M1), predominantly enriched in PLHIV-ART>1yr, and **b**, Module 2 (M2), enriched in PLHIV-ART<3m. Only pathways with a holm adjusted  $P < 0.05$  are shown. Abbreviations:  $-\log_{10}(\text{padj})$ ,  $-\log_{10}$  holm adjusted p-value.

**Supplementary Table S2:** Reagents and antibodies used for generating data in the manuscript.

Table shows reagents and antibodies used for a list of reagents that were used in the generation of data presented in this manuscript

Reagents used in the experiments shown in this manuscript		
Item	Manufacturer	Product code
Fetal Bovine Saline	Sigma-Aldrich	F9665-500ml
RPMI-1640 Medium (1X) with L Glutamine	Fisher Scientific	12004997
Penicillin-Streptomycin	Fisher Scientific	11548876
Gibco HEPES (1M)	Fisher Scientific	11560496
Gibco™ Phosphate Buffered Saline (PBS), pH7.2	Fisher Scientific	11540546
Nasosorption™ FX.1 working wavelength 400nm (HMD798)	Hunt Development (UK) Ltd	NSFL-FXI-11 (50)
LIVE/DEAD™ Fixable Far Red Dead Cell Stain Kit, for 633 or 635 nm excitation	Thermo Fisher Scientific	L10120

Antibodies and reactive dyes used for staining myeloid cells from nasal and peripheral blood cells		
Antibody	Supplier	Product code
FITC anti-human CD66b antibody	Biolegend	305104
PE anti-human CD63 antibody	Biolegend	353004
Brilliant Violet 421™ anti-human CD10 antibody	Biolegend	312218
Alexa Flour 700® anti-human CD11b antibody	Biolegend	301356
CD62L (L-selectin) Monoclonal antibody (OX85), eflour™660	eBiosciences	50-0623-82
PE/Cyanine7 anti-human CD14 antibody	Biolegend	325618
PerCP-Cy5.5 anti-human CD45 antibody	Biolegend	304028
Brilliant Violet 605™ anti-human CD326 (EpCAM) antibody	Biolegend	324224

Antibodies and reactive dyes used for staining lymphocytes from nasal and peripheral blood cells		
Antibody	Supplier	Product code
APC/Cy7 anti-human CD3 Antibody	Biolegend	353408
PerCP-Cy5.5 anti-human CD4 antibody	Biolegend	344818
Alexa Flour 700® anti-human CD8	Biolegend	331208
BD Pharmingen™ PE-Cy7 Mouse Anti-human CD56 (NCAM-1)	BD Biosciences	557747
PE/Dazzle™ 594 anti-human CD161 antibody	Biolegend	339940
PE anti-human TCR $\alpha$ 7.2	Biolegend	351706
FITC anti-human TCR $\gamma$ $\delta$	Biolegend	331208